

## Temperature and Pressure Dependence of the Rate Constant for the HO<sub>2</sub> + NO Reaction

John V. Seeley,<sup>†</sup> Roger F. Meads, Matthew J. Elrod, and Mario J. Molina\*

Department of Earth, Atmospheric and Planetary Sciences, and Department of Chemistry,  
Massachusetts Institute of Technology, Cambridge, Massachusetts 02139

Received: August 30, 1995; In Final Form: December 4, 1995<sup>⊗</sup>

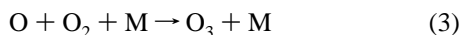
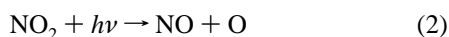
The rate constant for the reaction HO<sub>2</sub> + NO → OH + NO<sub>2</sub> has been measured using the turbulent flow technique with high-pressure chemical ionization mass spectrometry for the detection of reactants and products. At room temperature, the rate constant was found to be independent of pressure between 70 and 190 Torr of N<sub>2</sub> and given by  $(8.0 \pm 0.5) \times 10^{-12} \text{ cm}^3 \text{ molecule}^{-1} \text{ s}^{-1}$ . The temperature dependence of the rate constant was investigated between 206 and 295 K; the Arrhenius expression over this temperature range is  $(3.0 \pm 0.4) \times 10^{-12} \exp[(290 \pm 30)/T] \text{ cm}^3 \text{ molecule}^{-1} \text{ s}^{-1}$ . The uncertainties of the room temperature rate constant and the Arrhenius parameters represent the precision of the data and are reported at the 1 standard deviation level. We estimate that possible systematic errors limit the accuracy of the determined rate constants to  $\pm 15\%$ . Comparison of our data with the results of previous studies indicates that the rate constant for the HO<sub>2</sub> + NO → OH + NO<sub>2</sub> reaction does not depend on the inert gas pressure for 295 K  $\geq T \geq$  206 K.

### Introduction

Catalytic cycles determine to a large extent the concentration of ozone in the stratosphere. The cycle involving HO<sub>x</sub> radicals is the dominant removal mechanism of ozone in the mid-latitude stratosphere.<sup>1,2</sup> The effectiveness of this cycle is moderated by the reaction:



The importance of this reaction for stratospheric chemistry became apparent with the pioneering studies of Howard and Evenson,<sup>3</sup> who carried out the first direct measurements of its rate constant obtaining a value more than an order of magnitude larger than the value previously derived from indirect studies. Reaction 1 also plays a significant role in the troposphere, where it leads to ozone production when combined with the reactions:



Previous experimental studies have shown that reaction 1 has a rate constant that increases with decreasing temperature. This type of behavior in bimolecular reactions often indicates a complex mode reaction: a reaction involving multiple transition states and the formation of bound intermediates. Complex mode reactions can have rate constants which depend upon total pressure if the lifetime of the intermediate complex is sufficiently long to suffer collisions with the bath gas before going on to form the final products. Examples of complex-mode reactions with pressure dependencies include OH + CO, HO<sub>2</sub> + HO<sub>2</sub>, and OH + HNO<sub>3</sub>. The intermediate complex of reaction 1 would most likely be peroxyxynitrous acid, HOONO. This species has been observed in matrix isolation studies;<sup>4</sup> however, it has never been successfully detected in the gas phase.<sup>5</sup>

All previous direct determinations of the rate constant of reaction 1 have been carried out in conventional discharge flow tubes which are limited to pressures below 15 Torr and usually

to temperatures roughly above 240 K. As a result, the pressure dependence of the rate constant for reaction 1 remained uncertain.

In this article we describe our investigations of the kinetics of reaction 1 over a broad range of temperatures and pressures using a turbulent flow tube coupled to a high-pressure chemical ionization mass spectrometer. We have previously shown that the turbulent flow tube technique can be used to accurately determine the rate constants of reactions at pressures ranging from 50 to 760 Torr and at temperatures as low as 180 K.<sup>6,7</sup> In order to study reaction 1 we have developed a new detection system involving high-pressure chemical ionization mass spectrometry, which can be used to monitor HO<sub>2</sub>, OH, and NO<sub>2</sub> with high sensitivity.

### Experimental Section

**General Overview of the Experimental Apparatus.** A schematic of the experimental apparatus is shown in Figure 1. The flow tube was constructed with 2.2 cm id Pyrex tubing and was 120 cm in total length. A large flow of nitrogen carrier gas (approximately 50 L(STP) min<sup>-1</sup>) was injected at the rear of the flow tube. The gases necessary to generate HO<sub>2</sub> were also introduced at the rear of the flow tube. Nitric oxide was injected through a movable inlet constructed from 5 mm od stainless steel tubing. The portion of the inlet outside of the flow tube was encased in collapsible Teflon tubing. This provision was taken so the inlet could be moved to various axial positions without breaking any vacuum seals. A fan-shaped Teflon piece (a "turbulizer"), designed to enhance turbulent mixing, was fixed to the end of the movable inlet. The ion source was positioned 15 cm from the end of the flow tube. A quadrupole mass spectrometer (Balzers QMG 400) was located at the end of the flow tube. The flowing gases were removed with a rotary vane vacuum pump (Edwards E2M 80, 1600 L min<sup>-1</sup>). All gas flows were monitored with calibrated mass flow meters (Tylan). The pressure was determined immediately upstream of the ion source using a 0–1000 Torr capacitance manometer (MKS Baratron). The temperature was determined using copper–constantan thermocouples located at the rear of the flow tube, at the end of the movable inlet, and immediately upstream of the ion source.

<sup>†</sup> Current address: Ionospheric Effects Division, PL/GPID, Phillips Laboratory, 29 Randolph Rd., Hanscom AFB, MA 01731-3010.

<sup>⊗</sup> Abstract published in *Advance ACS Abstracts*, February 1, 1996.

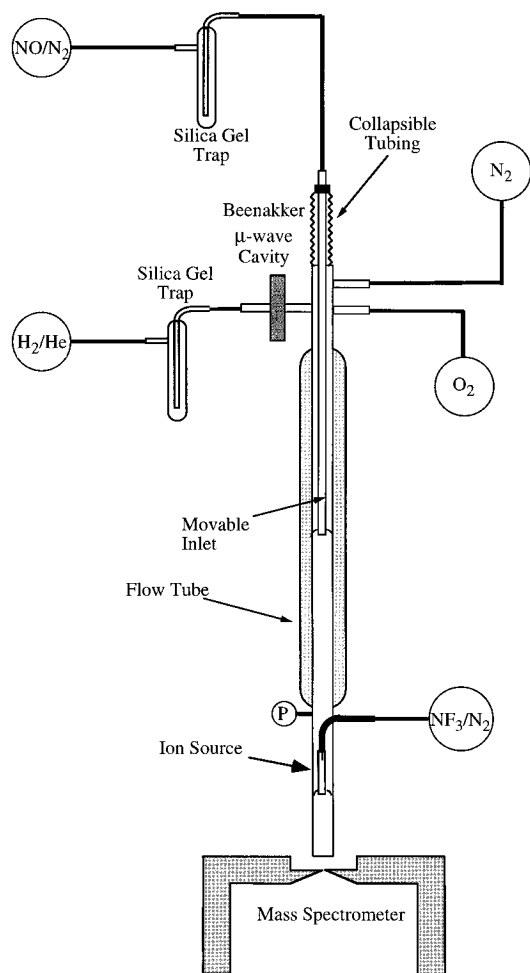


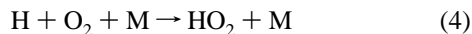
**Figure 1.** Schematic of the experimental apparatus.

All of the experiments were performed in turbulent flow conditions. Turbulent flow is established when the Reynolds number,  $Re$ , is greater than 2000. This number is given by

$$Re = \frac{2a\bar{u}\rho}{\mu}$$

where  $a$  is the internal radius of the flow tube,  $\bar{u}$  is the average velocity of the gas,  $\rho$  is the density of the gas, and  $\mu$  is the viscosity coefficient of the gas.

**Generation of Reactants.** HO<sub>2</sub> was produced in the rear portion of the flow tube via



Hydrogen atoms were generated in the following manner: A 2 L(STP) min<sup>-1</sup> flow of He (Airco Grade 5) was combined with a 0.2 mL(STP) min<sup>-1</sup> flow of a 1% H<sub>2</sub>/He mixture (Air Products UHP). The resulting mixture was passed through a silica gel trap immersed in liquid nitrogen and then through a microwave discharge produced by a Beenakker cavity operating at 70 W. The microwave discharge dissociated some of the H<sub>2</sub> molecules into hydrogen atoms. The H atoms were then injected into the flow tube through a side-arm inlet located near the rear of the flow tube. Oxygen (Matheson UHP) was injected into the flow tube 3 cm downstream of the H-atom injection point. The density of O<sub>2</sub> in the flow tube was approximately 10<sup>15</sup> molecules cm<sup>-3</sup>. The end of the movable inlet was always further than 40 cm downstream of the O<sub>2</sub> injection point. At the pressures and velocities used in this study, we calculate that the H + O<sub>2</sub> reaction went to greater than 99% completion before reaching the tip of the movable inlet. H atoms were periodically titrated

with NO<sub>2</sub> to determine their concentration after injection into the flow tube, as follows: the O<sub>2</sub> was replaced with a known quantity of NO<sub>2</sub> (Matheson, 99.5%), normally near 3 × 10<sup>11</sup> molecules cm<sup>-3</sup>. The mass spectrometer signal from NO<sub>2</sub> was then monitored with the microwave discharge turned off and then on. The decrease in the NO<sub>2</sub> signal that was observed was attributed to



Our calculations show that reaction 5 should proceed to greater than 98% completion before reaching the ion source. Using this method we found that on average 15% of the H<sub>2</sub> was dissociated into H atoms. Under normal operating conditions the initial concentration of hydrogen atoms in the flow tube was approximately 1 × 10<sup>11</sup> molecules cm<sup>-3</sup>.

Purified NO/N<sub>2</sub> mixtures were prepared by the following process: First, NO (Matheson CP grade) was condensed in a cold finger at 77 K. The resulting crystals were evacuated to remove volatile impurities (i.e., O<sub>2</sub>, N<sub>2</sub>, etc.). After 5 min of pumping, the cold finger was isolated from the pump and warmed to 143 K (pentane slush) which vaporized the NO while leaving other oxides of nitrogen still in the condensed phase. The desired amount of NO was then mixed with N<sub>2</sub> (Airco Grade 5) and stored in a stainless steel cylinder. Before being injected into the flow tube, the NO mixture was further diluted with a 200 mL(STP) min<sup>-1</sup> flow of N<sub>2</sub> and then passed through a silica gel trap at 195 K (ethanol slush). The concentration of NO in the flow tube was determined from calibrated mass flow meter readings and ranged from 1 × 10<sup>12</sup> to 15 × 10<sup>12</sup> molecules cm<sup>-3</sup>. In all cases [NO] ≫ [HO<sub>2</sub>], thus ensuring pseudo-first-order conditions.

**Detection of Reactants and Products.** HO<sub>2</sub>, OH, and NO<sub>2</sub> were chemically ionized with selected reagent ions and then detected with the mass spectrometer. The reagent ions were produced in the ion source by passing approximately 10 ppm of ion precursor (NF<sub>3</sub> or SF<sub>6</sub>) over the corona discharge. The ion precursor was carried by a 10 L(STP) min<sup>-1</sup> flow of N<sub>2</sub>. The corona discharge took place at the end of a steel needle that was maintained at an electrical potential of -4000 V using a Bertan high-voltage power supply. The discharge current was approximately 30 μA. An electrically grounded 6 mm od stainless steel tube served as the counter electrode. The needle was separated from the stainless steel tube with a 3 mm od glass tube. After passage over the needle, the ion source gas was directed through a 5 cm long Pyrex tube and then into the main flow tube. A turbulizer was placed at the end of the small Pyrex tube to help the reagent ions mix with the main flow tube gas. The end of the ion injector tube was 7 cm from the front aperture of the mass spectrometer.

Ions were detected with a quadrupole mass spectrometer housed in a two-stage differentially pumped vacuum chamber. Flow tube gases (neutrals and ions) were drawn into the front chamber through a 0.1 mm aperture which was held at a potential of -130 V. The ions were focused by three lenses constructed from 3.8 cm id, 4.8 cm od copper gaskets. The front vacuum chamber was pumped by a 6 in. diffusion pump (Varian VHS-6, 2400 L s<sup>-1</sup>) backed by a mechanical pump (Varian SD-700, 765 L min<sup>-1</sup>). When the flow tube was at a pressure of 100 Torr, the front chamber pressure was roughly 5 × 10<sup>-6</sup> Torr. The sampled gases entered the rear vacuum chamber through a skimmer cone with a 1.2 mm orifice (Beam Dynamics Model 2). The distance between the front aperture and the skimmer cone was approximately 5 cm. The skimmer cone was held at a potential of -20 V. Once the ions passed through the skimmer cone, they were mass filtered and detected with a Balzers QMG 400 quadrupole mass spectrometer. The

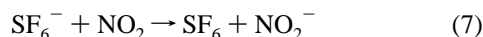
rear vacuum chamber was pumped by a turbomolecular pump (Edwards EXT 501,  $500 \text{ L s}^{-1}$ ) backed by a mechanical pump (Edwards E2M 12,  $289 \text{ L min}^{-1}$ ). When the flow tube was at a pressure of 100 Torr, the rear chamber pressure was roughly  $5 \times 10^{-7}$  Torr.

Two reagent ions were used in this study:  $\text{F}^-$  and  $\text{SF}_6^-$ . Fluorine anions were produced by passing trace amounts of  $\text{NF}_3$  (Air Products, electronic grade) over the corona. A typical density of  $\text{NF}_3$  injected into the flow tube was  $1 \times 10^{13}$  molecules  $\text{cm}^{-3}$ . The signal at 19 amu ( $\text{F}^-$ ) was approximately 50 000 counts  $\text{s}^{-1}$ . Smaller quantities of fluorine hydrates ( $\text{F}^- \cdot \text{H}_2\text{O}$ , and  $\text{F}^- \cdot 2\text{H}_2\text{O}$ ) were also produced.  $\text{SF}_6^-$  ions were generated by passing trace amounts of  $\text{SF}_6$  (Matheson, CP Grade) over the corona discharge. A typical density of  $\text{SF}_6$  injected into the flow tube was  $5 \times 10^{12}$  molecule  $\text{cm}^{-3}$ . The signal at 146 amu ( $\text{SF}_6^-$ ) was approximately 300 000 counts  $\text{s}^{-1}$ .

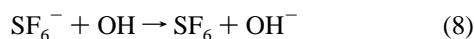
$\text{HO}_2$  was detected as  $\text{O}_2^-$  by the proton transfer reaction



Reaction 6 has not yet been directly studied; however, the reaction is exothermic by approximately  $20 \text{ kcal mol}^{-1}$ .<sup>8</sup>  $\text{NO}_2$  was detected as  $\text{NO}_2^-$  using the charge transfer reaction with  $\text{SF}_6^-$ :



The rate constant of reaction 7 has been measured by Streit<sup>9</sup> to be  $1.3 \times 10^{-10} \text{ cm}^3 \text{ molecule}^{-1} \text{ s}^{-1}$ .  $\text{OH}$  was detected through a two-step chemical ionization scheme. The first step is charge transfer with  $\text{SF}_6^-$ :



The rate constant of reaction 8 has been estimated by Lovejoy et al.<sup>10</sup> to be  $2 \times 10^{-9} \text{ cm}^3 \text{ molecule}^{-1} \text{ s}^{-1}$ . The second step is:



Reaction 9 has been reported by Fehsenfeld and Ferguson<sup>11</sup> to have a rate constant of  $8.6 \times 10^{-28} \text{ cm}^6 \text{ molecule}^{-2} \text{ s}^{-1}$ . We found that the  $\text{HCO}_3^-$  signal was proportional to  $[\text{OH}]$ . A maximum signal to noise ratio was obtained when approximately  $2 \times 10^{14}$  molecules  $\text{cm}^{-3}$  of  $\text{CO}_2$  (Matheson, 99.8%) was injected into the flow tube at a position immediately upstream of the ion source. We found that using the first step alone yields an  $\text{OH}^-$  signal which is nonlinear with  $[\text{OH}]$ , most likely due to secondary reactions.

**Temperature Control.** The temperature of the reaction region (the area between the end of the movable inlet and the ion source) was controlled to within 1 K. The walls of the flow tube were cooled to the desired temperature by flowing a temperature-controlled liquid (either ethanol or HCFC-123) through the jacket on the exterior of the flow tube. The nitrogen carrier gas was precooled to the desired temperature by passage through a copper coil immersed in the temperature-controlled liquid before injection into the flow tube.

## Results and Discussion

**Assessment of Detector Sensitivity.** Trace quantities of  $\text{NO}_2$ ,  $\text{HO}_2$ , and  $\text{OH}$  were individually injected into the flow tube in order to calibrate the mass spectrometer signals. Dilute mixtures of  $\text{NO}_2$  were injected at the rear of the flow tube through the port normally used for  $\text{O}_2$  injection; a plot of the  $\text{NO}_2^-$  signal vs  $[\text{NO}_2]$  is shown in Figure 2a. At a flow tube pressure of 100 Torr, we estimate that  $5 \times 10^8$  molecules  $\text{cm}^{-3}$

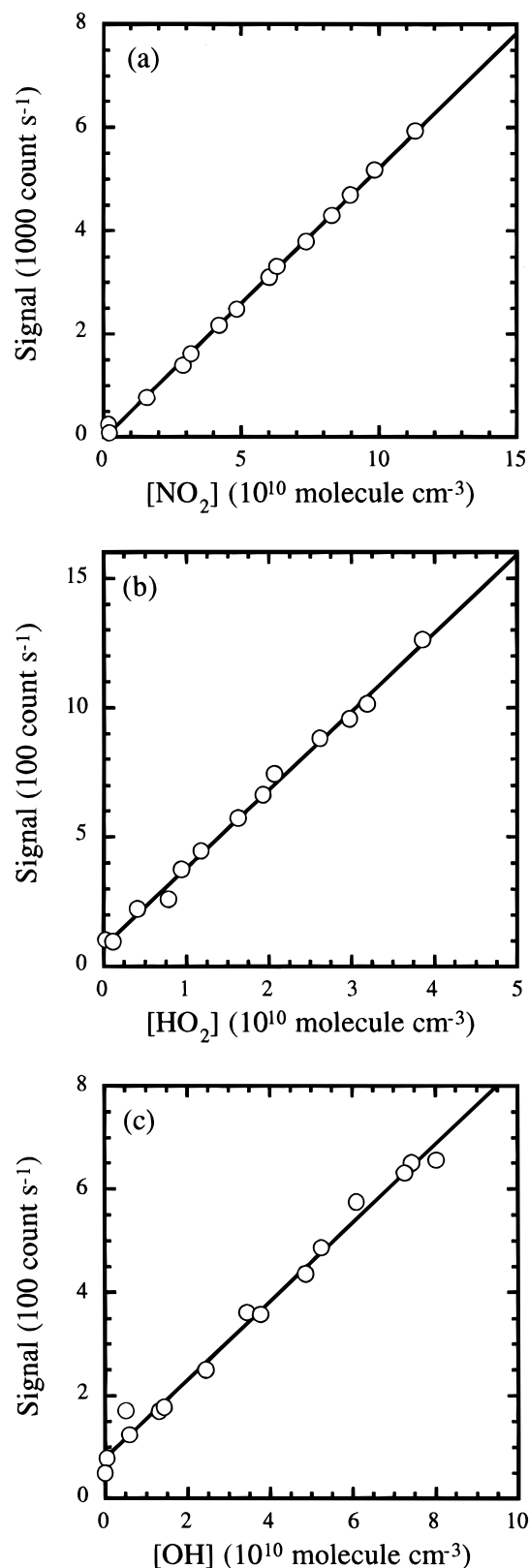


**Figure 2.** (a) Signal intensity at 46 amu ( $\text{NO}_2^-$ ) as a function of  $\text{NO}_2$  concentration. Data points were collected under the following flow tube conditions:  $P = 100$  Torr;  $T = 292$  K; average velocity =  $1300 \text{ cm s}^{-1}$ ;  $Re = 3000$ . (b) Signal intensity at 32 amu ( $\text{O}_2^-$ ) as a function of  $\text{HO}_2$  concentration. Data points were collected under the following flow tube conditions:  $P = 96$  Torr;  $T = 292$  K; average velocity =  $1430 \text{ cm s}^{-1}$ ;  $Re = 2600$ . (c) Signal intensity at 61 amu ( $\text{HCO}_3^-$ ) as a function of  $\text{OH}$  concentration. Data points were collected under the following flow tube conditions:  $P = 96$  Torr;  $T = 292$  K; average velocity =  $1430 \text{ cm s}^{-1}$ ;  $Re = 2600$ .

of  $\text{NO}_2$  yield a signal to noise ratio equal to 1. This corresponds to 0.1 ppb detection limit (at 100 Torr).

The concentration of HO<sub>2</sub> was estimated as described in the experimental section; it was assumed that the microwave discharge dissociated 15% of the H<sub>2</sub> into H atoms, which were then converted into HO<sub>2</sub> via reaction 4. A plot of the O<sub>2</sub><sup>-</sup> signal vs [HO<sub>2</sub>] is shown in Figure 2b. We found that such plots were linear when [HO<sub>2</sub>] was less than 3 × 10<sup>11</sup> molecules cm<sup>-3</sup>. The positive intercept is due to HO<sub>2</sub> produced by residual H<sub>2</sub> in the silica gel trap. The magnitude of this intercept was found to slowly decrease after the H<sub>2</sub> was shut off. At a flow tube pressure of 100 Torr, we estimate that [HO<sub>2</sub>] = 1 × 10<sup>9</sup> molecules cm<sup>-3</sup> produces a signal to noise ratio equal to 1. As the flow tube pressure was raised, the sensitivity decreased due to increased clustering of F<sup>-</sup> with water. At pressures above 200 Torr we estimate that the sensitivity was reduced by approximately a factor of 3.

OH was produced by reaction 5. Hydrogen atoms were injected at the rear of the flow tube, and NO<sub>2</sub> was injected through the O<sub>2</sub> port. The NO<sub>2</sub> concentration in the flow tube was approximately 5 × 10<sup>11</sup> molecules cm<sup>-3</sup>. The concentration of OH was estimated by assuming that the microwave discharge dissociated 15% of the H<sub>2</sub> into H atoms and that all of the H atoms were converted into OH by reaction 5. A plot of the HCO<sub>3</sub><sup>-</sup> signal vs [OH] is shown in Figure 2c. The positive intercept is due to OH produced by residual H<sub>2</sub> in the silica gel trap. At a flow tube pressure of 100 Torr, we estimate that [OH] = 5 × 10<sup>9</sup> molecules cm<sup>-3</sup> produces a signal to noise ratio equal to 1.

For the cases of NO<sub>2</sub> and HO<sub>2</sub>, the chemical ionization technique provides greater sensitivity than other flow tube detection techniques commonly employed in the past. For example, electron impact mass spectrometry for NO<sub>2</sub> is frequently reported to have a sensitivity on the order of 100 ppb,<sup>12</sup> which is roughly 3 orders of magnitude less sensitive than the chemical ionization scheme employed in this work. The most successful flow tube detection technique for HO<sub>2</sub> is laser magnetic resonance (LMR); Howard<sup>13</sup> reports a detection limit of 4 × 10<sup>8</sup> molecules cm<sup>-3</sup> of HO<sub>2</sub> at pressures near 1 Torr of He with this technique. However, LMR sensitivity is approximately inversely proportional to the square of the total pressure due to line broadening.<sup>14</sup> Thus, at pressures high enough for turbulent flow (*P* > 50 Torr), LMR would be at least an order of magnitude less sensitive than the chemical ionization detection technique. For the case of OH, our chemical ionization detection scheme is not as sensitive as the commonly used laser induced fluorescence (LIF) detection technique; e.g., Abbatt et al.<sup>15</sup> report LIF detection limits of 2 × 10<sup>8</sup> molecules cm<sup>-3</sup> for OH in 100 Torr of N<sub>2</sub>, which is at least 1 order of magnitude more sensitive than our chemical ionization detection technique. However, it should be noted that chemical ionization mass spectrometry has been used to detect OH in the atmosphere at sub-parts per trillion levels;<sup>16</sup> thus, it is likely that an improved chemical ionization scheme will enable much greater sensitivity for OH in laboratory flow tube studies.

**Determination of Rate Constants.** The rate constant of reaction 1 was determined as follows: first, the NO mixture was injected at a predetermined rate, and [NO] was calculated by assuming complete mixing in the region downstream of the movable inlet. The O<sub>2</sub><sup>-</sup> signal intensity was then recorded as a function of the movable injector position. The logarithm of the measured signal intensity was then plotted as a function of injector–detector distance. The data points were fitted with a linear least squares routine. The value of the pseudo-first-order rate constant, *k*<sup>l</sup>, was determined by multiplying the resulting slope by the average gas velocity. This process was repeated for approximately 10 different concentrations of NO; Figure 3

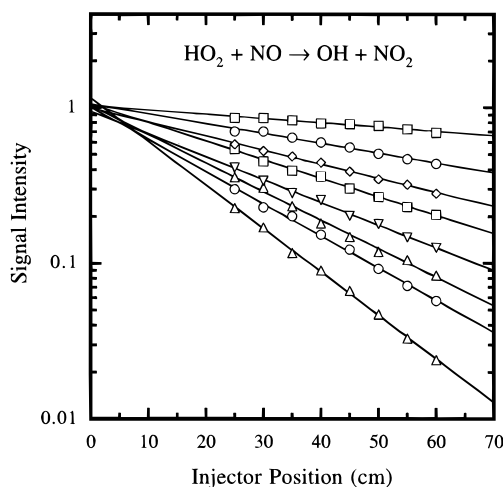


**Figure 3.** Typical set of O<sub>2</sub><sup>-</sup> signal values as a function of injector position. This data set was obtained under the following conditions: *P* = 149 Torr; *T* = 292 K; average velocity = 1235 cm s<sup>-1</sup>; *Re* = 3550.

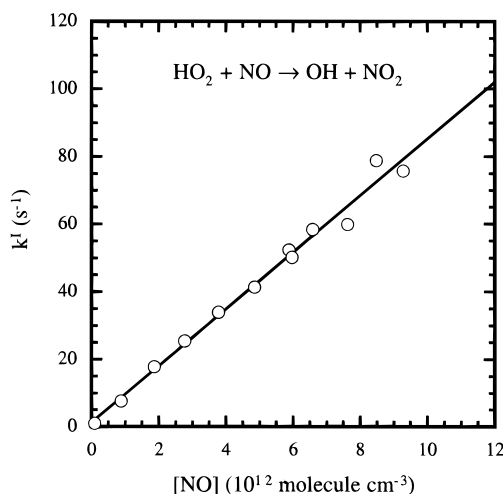


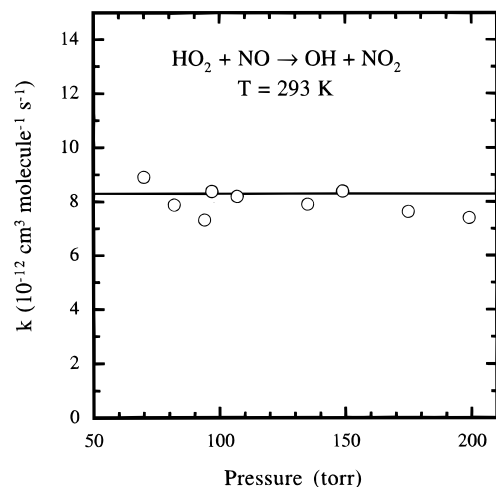
**Figure 4.** Typical plot *k*<sup>l</sup> as a function of [NO]. This data set was obtained under the following conditions: *P* = 149 Torr; *T* = 292 K; average velocity = 1235 cm s<sup>-1</sup>; *Re* = 3550.

shows a portion of a typical data set. Such plots were essentially linear for all of the experiments, indicating that secondary reactions occurred to a minimal extent. The *k*<sup>l</sup> values were then plotted vs [NO], and the data points were fitted with a linear least squares routine, the slope of the fit provided the bimolecular rate constant, *k*. Figure 4 shows a typical plot of *k*<sup>l</sup> vs [NO]. We estimate that rate constants can be determined with an accuracy of ±15%, considering possible systematic errors in the measurement of gas flows, temperature, detector signal, and pressure.

The approach for determining rate constants described above assumes that deviations from plug flow are negligible. The validity of this assumption was examined with two-dimensional numerical flow tube model.<sup>17</sup> For the flow simulation we assumed that the detection technique samples the entire cross section of the flow tube. This is a reasonable assumption because the flow is thoroughly mixed by the ion source turbulizer immediately before sampling. We also assumed that the reaction probability of HO<sub>2</sub> on the walls, *γ*, is 10<sup>-4</sup>, on the basis of experimental results for the loss of HO<sub>2</sub> on the walls of similar flow tubes.<sup>3,18</sup> Using these assumptions, the model predicts that the plug flow approximation yields rate constants which are 3% lower than the actual rate constant. This deviation is small when compared with our estimated uncertainty of ±15% due to errors in the measurement of gas flows, temperature, detector signal, and pressure. The deviation from plug flow

**TABLE 1: Summary of Rate Constants for Reaction 1 Obtained at Temperatures around 295 K**

$T$ (K)	$P$ (Torr)	velocity (cm s <sup>-1</sup> )	$Re$	$k \pm \sigma$ (10 <sup>-12</sup> cm <sup>3</sup> s <sup>-1</sup> )
292	70	2397	3231	8.92 ± 0.42
294	82	1717	2660	7.89 ± 0.27
294	94	1404	2530	7.33 ± 0.24
295	97	1605	2960	8.39 ± 0.28
293	107	1375	2800	8.21 ± 0.39
292	135	1164	3030	7.92 ± 0.18
292	149	1235	3550	8.40 ± 0.31
295	175	1035	3440	7.64 ± 0.28
291	199	910	3520	7.41 ± 0.35

**Figure 5.** Plot of the HO<sub>2</sub> + NO rate constant as a function of flow tube pressure. Each point was obtained at a temperature near 293 K. The solid line represents the average of the previously reported values,  $8.3 \times 10^{-12} \text{ cm}^3 \text{ molecule}^{-1} \text{ s}^{-1}$  (see Table 2).

increases as the walls become more reactive: the rate constants determined using the plug flow approximation are predicted by the model to be accurate to within 2% in the absence of wall reactions ( $\gamma = 0$ ) and to within 8% assuming that HO<sub>2</sub> molecules are removed with every wall collision ( $\gamma = 1$ ).<sup>19</sup>

The rate constant for reaction 1 was determined at flow tube pressures ranging from 70 to 190 Torr. Table 1 contains a summary of the rate constants determined near room temperature; these results are also shown in Figure 5. As can be seen in the figure, the rate constant is independent of pressure to within experimental error. The average value of the rate constant near 294 K is  $k = (8.0 \pm 0.5) \times 10^{-12} \text{ cm}^3 \text{ molecule}^{-1} \text{ s}^{-1}$ ; the uncertainty represents the scatter in the data at the 1 standard deviation level and is not an estimate of systematic errors. If a linear fit is made to the data, the following expression is  $k = [(8.7 \pm 0.5) - (0.006 \pm 0.005)P] \times 10^{-12} \text{ cm}^3 \text{ molecule}^{-1} \text{ s}^{-1}$ , where  $P$  is the flow tube pressure in Torr.

The average value of the rate constant determined in this work is in excellent agreement with the results of previous low-pressure flow tube studies. A summary of the previous measurements of the rate constant near room temperature is listed in Table 2.

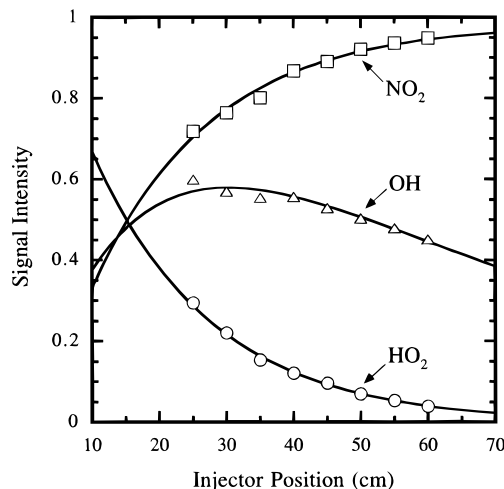
In several cases the products of reaction 1 were also monitored. Figure 6 shows a plot of the HO<sub>2</sub>, NO<sub>2</sub>, and OH signals as a function of injector position. The curve passing through the HO<sub>2</sub> and NO<sub>2</sub> data represents the values calculated for a first-order decay of reactants and a first-order appearance of products, respectively. Although OH is a product of reaction 1, the OH signal slowly decays as the injector is pulled back due to the secondary reaction with NO:



The curve passing through the OH data is based on the combined

**TABLE 2: Summary of Experimental Determinations of the Rate Constant of Reaction 1**

$k \pm \sigma$ (10 <sup>-12</sup> cm <sup>3</sup> s <sup>-1</sup> )	$T$ (K)	pressure range	ref
8.1 ± 0.8	296	1.1–1.7 Torr of He	3
8 ± 1	298	1.0 Torr of He	20
7.9 ± 0.5	298	1.0 Torr of He	21
8.0 ± 0.5	296	0.9 Torr of He	13
9.0 ± 1.4	298	2 Torr of He	12
11 ± 2	297	0.75–1.2 Torr of He	22
7.6 ± 0.9	293	2–12 Torr of He	23
6.9 ± 0.3	298	2 Torr of Ar	24
8.5 ± 0.7	297	0.8–13 Torr of N <sub>2</sub>	25
8.0 ± 0.5	294	70–199 Torr of N <sub>2</sub>	this work

**Figure 6.** Signal intensity as a function of injector position. The curve passing through the HO<sub>2</sub> and NO<sub>2</sub> data represents the values calculated for a first-order decay of reactants and a first-order appearance of products, respectively. The curve passing through the OH data is based on the combined effect of reaction 1 and reaction 10 on the OH concentration. The data points were obtained under the following flow tube conditions:  $P = 108$  Torr;  $T = 294$  K; average velocity = 1420 cm s<sup>-1</sup>;  $Re = 2930$ .**TABLE 3: Summary of Rate Constants for Reaction 1 Obtained in the Temperature Range 295 K >  $T$  > 200 K**

$T$ (K)	$P$ (Torr)	velocity (cm s <sup>-1</sup> )	$Re$	$k \pm \sigma$ (10 <sup>-12</sup> cm <sup>3</sup> s <sup>-1</sup> )
293	107	1375	2800	8.21 ± 0.78
280	97	1695	3400	9.08 ± 0.80
280	92	1570	3040	7.71 ± 0.44
269	98	1690	3720	8.84 ± 0.52
260	97	1460	3370	9.44 ± 0.36
253	96	1505	3610	8.69 ± 0.46
252	85	1410	3040	9.86 ± 0.57
243	94	1490	3760	9.53 ± 0.21
235	93	1405	3685	11.4 ± 0.5
234	95	1423	3890	10.2 ± 0.5
224	91	1375	3870	10.7 ± 0.4
224	95	1445	4260	11.7 ± 0.5
220	93	1450	4300	10.5 ± 0.5
215	93	1280	3980	12.2 ± 0.8
211	99	1750	5950	11.8 ± 0.5
206	94	1275	4300	12.0 ± 0.5

effect of reaction 1 and reaction 10 on the OH concentration assuming  $k_{10} = 7.0 \times 10^{-31} \text{ cm}^3 \text{ molecule}^{-1} \text{ s}^{-1}$ .<sup>26</sup>

We also measured the rate constant for reaction 1 at temperatures between 206 and 293 K. A summary of these results is given in Table 3 and in Figure 7. The majority of the rate constants were determined at a pressure of approximately 95 Torr. The rate constant was observed to increase by approximately 50% as the temperature was lowered from 300 to 200 K. From the data listed in Table 3, we obtain the Arrhenius expression  $k(T) = (3.0 \pm 0.4) \times 10^{-12} \exp[(290 \pm 30)/T] \text{ cm}^3 \text{ molecule}^{-1} \text{ s}^{-1}$ ; the uncertainty is given at the 1 standard deviation level. Howard<sup>13</sup> has performed the only other

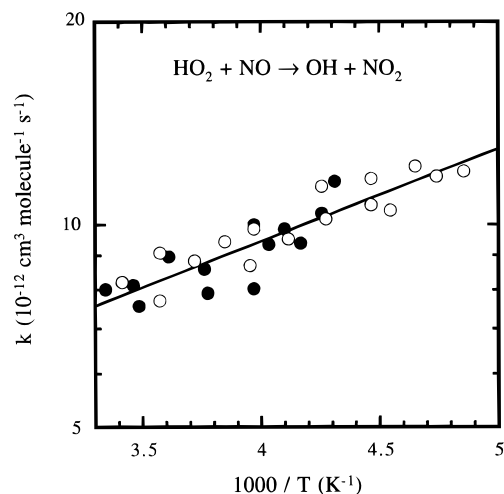


**Figure 7.** Arrhenius plot for the reaction HO<sub>2</sub> + NO. The open circles are experimental data from this work, and the line is the resulting Arrhenius fit. The data of Howard<sup>13</sup> are represented by filled circles.

through temperature dependence study for  $T < 300$  K; a comparison of his results with the results of this study is also shown in Figure 7. Given the close agreement between Howard's low pressure results and our higher pressure values, we conclude that the rate constant does not have a significant pressure dependence for temperatures between 200 and 300 K. If Howard's data set is combined with our data set, an Arrhenius expression of  $(2.67 \pm 0.31) \times 10^{-12} \exp[(316 \pm 30)/T]$  cm<sup>3</sup> molecule<sup>-1</sup> s<sup>-1</sup> is obtained.

The negative temperature dependency for the rate constant for reaction 1 indicates that the reaction proceeds through the formation of an intermediate; the absence of a measurable pressure dependency points out that such an intermediate is too short-lived to be affected by collisions with the carrier gas. The magnitude of a possible pressure effect is expected to increase as the temperature is lowered; however, we see no evidence for such an effect down to 200 K. It is also possible that species such as water vapor or oxygen give rise to a pressure effect which is larger than that due to nitrogen, as is the case, for example, with the HO<sub>2</sub> self-reaction.<sup>26</sup> Additional studies of such pressure effects would be useful.

## Conclusions

Our data indicate that reaction 1 does not have a substantial pressure dependence at temperatures between 200 and 300 K. Our results are in excellent agreement with previous results obtained in low-pressure discharge flow systems. This work also shows that key radical species, such as HO<sub>2</sub> and OH, can be monitored using chemical ionization mass spectrometry with greater sensitivity than that provided by conventional electron impact mass spectrometers; work in progress in our laboratory also indicates that many stable species can be monitored as well with superb sensitivity. Furthermore, our results show that high-pressure chemical ionization mass spectrometry can be suc-

cessfully coupled to turbulent flow tube systems for chemical kinetic studies at relatively high pressures and low temperatures, that is, under conditions outside the operating range of the well-established conventional fast flow technique.

**Acknowledgment.** The research described in this article was supported by a grant from the NASA Upper Atmospheric Research Program to the Massachusetts Institute of Technology.

## References and Notes

- (1) Wennberg, P. O.; Cohen, R. C.; Stimpfle, R. M.; Koplow, J. P.; Anderson, J. G.; Salawitch, R. D.; Fahey, D. W.; Woodbridge, E. L.; Keim, E. R.; Gao, R. S.; Webster, C. R.; May, R. D.; Toohey, D. W.; Avallone, L. M.; Proffitt, M. H.; Lowenstein, M.; Podolske, J. R.; Chan, K. R.; Wofsy, S. C. *Science* **1994**, *266*, 398.
- (2) Cohen, R. C.; Wennberg, P. O.; Stimpfle, R. M.; Koplow, J. P.; Anderson, J. G.; Fahey, D. W.; Woodbridge, E. L.; Keim, E. R.; Gao, R. S.; Proffitt, M. H.; Lowenstein, M.; Chan, K. R. *Geophys. Res. Lett.* **1994**, *21*, 2539.
- (3) Howard, C. J.; Evenson, K. M. *Geophys. Res. Lett.* **1977**, *4*, 437.
- (4) Cheng, B. M.; Lee, J. W.; Lee, Y. P. *J. Phys. Chem.* **1991**, *95*, 2814.
- (5) Burkholder, J. B.; Hammer, P. D.; Howard, C. J. *J. Phys. Chem.* **1987**, *91*, 2136.
- (6) Seeley, J. V.; Jayne, J. T.; Molina, M. J. *Int. J. Chem. Kinet.* **1993**, *25*, 571.
- (7) Seeley, J. V.; Jayne, J. T.; Molina, M. J. Submitted for publication.
- (8) Harrison, A. G. *Chemical Ionization Mass Spectrometry*, 2nd ed., CRC Press: Boca Raton, FL, 1992.
- (9) Streit, G. E. *J. Chem. Phys.* **1982**, *77*, 826.
- (10) Lovejoy, E. R.; Murrells, T. P.; Ravishankara, A. R.; Howard, C. J. *J. Phys. Chem.* **1990**, *94*, 2386.
- (11) Fehsenfeld, F. C.; Ferguson, E. E. *J. Chem. Phys.* **1974**, *61*, 3181.
- (12) Leu, M. T. *J. Chem. Phys.* **1979**, *70*, 1662.
- (13) Howard, C. J. *J. Chem. Phys.* **1979**, *71*, 2352.
- (14) Jemi-Alade, A. A.; Thrush, B. A. *J. Chem. Soc., Faraday Trans.* **1990**, *86*, 3355.
- (15) Abbatt, J. P. D.; Demerjian, K. L.; Anderson, J. G. *J. Phys. Chem.* **1990**, *94*, 4566.
- (16) Eisele, F. L.; Tanner, D. J. *J. Geophys. Res.* **1991**, *96*, 9295.
- (17) (a) Seeley, J. V.; Molina, M. J. Manuscript in preparation for submission to *Int. J. Chem. Kinet.* (b) Seeley, J. V. Experimental Studies of Gas Phase Radical Reactions Using the Turbulent Flow Tube Technique, Ph.D. Thesis, MIT, 1994.
- (18) Chang, J. S.; Kaufmann, F. *J. Phys. Chem.* **1978**, *82*, 1683.
- (19) Previously, we have reported that in turbulent flow conditions the plug flow approximation yields rate constants which are approximately 12% less than the actual value.<sup>6,7,17</sup> In these cases the greater predicted deviation was a result of using a detection technique (resonance fluorescence) which preferentially samples the faster moving central portion of the flow tube cross section.
- (20) Margitan, J. J.; Anderson, J. G. Results presented at 13th Informal Conference on Photochemistry, Clearwater Beach, FL, 1978.
- (21) Kaufman, F.; Reimann, B. Results presented at 13th Informal Conference on Photochemistry, Clearwater Beach, FL, 1978.
- (22) Glaschick-Schimpf, I.; Leiss, A.; Monkhouse, P. B.; Schurath, U.; Becker, K. H.; Fink, E. H. *Chem. Phys. Lett.* **1979**, *67*, 318.
- (23) Hack, W.; Preuss, W.; Temps, F.; Wagner, H. G. G. *Int. J. Chem. Kinet.* **1980**, *12*, 850.
- (24) Thrush, B. A.; Wilkinson, J. P. T. *Chem. Phys. Lett.* **1981**, *81*, 1.
- (25) Jemi-Alade, A. A.; Thrush, B. A. *J. Chem. Soc., Faraday Trans.* **1990**, *86*, 3355.
- (26) DeMore, W. B.; Sander, S. P.; Howard, C. J.; Ravishankara, A. R.; Golden, D. M.; Kolb, C. E.; Hampson, R. F.; Kurylo, M. J.; Molina, M. J. *Chemical Kinetics and Photochemical Data for Use in Stratospheric Modeling*; JPL Publication 94-26; Jet Propulsion Laboratory: Pasadena, CA, 1994.